Jestr

Journal of Engineering Science and Technology Review 17 (5) (2024) 117-125

Research Article

JOURNAL OF
Engineering Science and Technology Review

www.jestr.org

A Comparative Study of a High Gain Observer and a Nonlinear Observer based on the Circle Criterion for Sensorless Induction Motor Control

Abdelhak Benheniche[1], Farid Berrezzek[2] and Hacene Mellah[3,*]

[1]*Electromechanical Department, M.B. Ibrahimi University, Bordj Bou Arreridj 34000, Algeria*
[2]*Fac. Sci & Tec., LEER Lab.Univ. Med Cherif Messaadia University, Souk Ahras 41000, Algeria*
[3]*Electrical Engineering Department, Faculty of sciences and applied sciences, University of Bouira, 10000 Bouira, Algeria.*

Received 10 January 2024; Accepted 13 September 2024

Abstract

This paper compares between a High-Gain Observer (HGO) with a nonlinear observer based on the Circle Criteria Observer (CCO) for sensorless control of induction motor (IM) drives. The circle criterion method is better for making nonlinear observers because it doesn't require as strict conditions as other methods that try to get rid of system nonlinearities using a transformation nonlinear state. However, the high gain observer makes an effort to dominate the nonlinearities in the system with a high-gain output adjustment term. The suggested study uses the backstepping control method and looks at three performance criteria: tracking the trajectory, rejecting disturbances, and maintaining steady-state stability. It was found that the circle-based nonlinear estimator works better than the interconnected observer, based on the results and the comparison criteria already mentioned.

Keywords: Nonlinear observer, High-gain observer, Backstepping control, Induction motor, Lyapunov stability.

1. Introduction

Over the past decades, the field of sensorless control has become one of the most attractive areas of research in the control of electric actuators. This is due to the increased reliability and reduced cost of the system [1-2]. The essential elements of this domain are the electrical machine, the control strategy and the state observer. Due to their efficiency, effectiveness, simplicity, high reliability, resilience, and power density, asynchronous motors are the most commonly used machines in industries [3]. However, because of the rotor state-space variables and parameters of this motor are not measurable and it is nonlinear, highly linked, time fluctuating multivariate system, controlling, diagnosing, and monitoring is made more difficult [4]. To overcome the above problems and ensure the high performance of this machine, many types of nonlinear control approaches have been proposed and tested in practice. Among these strategies, we can cite the input-output linearization technique [5-6], sliding mode approach [7-8], Backstepping and Integral Backstepping method [9-11], flatness strategy [12-13] and adaptive algorithms [14-15] to solve the problem of time varying parameters. As mentioned above, Backstepping control is a nonlinear strategy widely used in a wide range of nonlinear systems that provides overall stabilization. On the other hand, it performs well even in the presence of variability. This technique is mainly based on the utilization of the Lyapunov function [15]. However, as with all nonlinear control techniques, it is necessary to have reliable and precise information on the various state variables of the system. In this situation, recourse to state-observers becomes an unavoidable solution. It should be noted that a state observer is a system that changes. Which can estimate the non-measurable state variables from the available measurements of the inputs and outputs of the considered system. This software sensor is crucial not only for control, but also for system monitoring, diagnostics, and fault tolerant control strategies.

Recently, a number of estimation techniques have been used to estimate IM rotor variables [16]. These approaches include the extended Kalman filter, which is a stochastic recursive estimation strategy for nonlinear systems [17]. Researchers often opt for this approach due to its ease of implementation and popularity in estimation [18]. The nonlinear Luenberger observer is distinguished by its inherent simplicity in comparison to the other approaches, without reducing estimate precision [19]. The Model Reference Adaptive System (MRAS) observer has become very popular in sensorless IM control because of its ease of implementation, good stability, low computational effort, and its good performance [20]. The Sliding Mode (SM) observer has the advantage of being unaffected by rotor time constant fluctuations [21]. Yet, they have the following limitations: the triangle block structures, the sensitivity against measurement noises, and the peaking phenomenon's disturbing influence.

The nonlinear observer constructed on the circle criterion introduced by Arckak and Kokotovich [22] allows for manipulation of the non-linearities directly and with less severe restrictions than the approaches of linearization and large gains [23-24]. Among the observers who have found a place in the sensorless control of electrical machines, we cite the High-Gain Observer (HGO) [25]. The use of these observers is motivated by their capacity to estimate in a robust way the unmeasured states while attenuating in an asymptotic way the disturbances [26-28]. However, the disadvantages of this observer are in their implementation, their calibration, and their very high gain which sometimes limit their use [29-30]. Motivated by the characteristics of the observers cited above, in this paper, we compare the HGO and the observer using the circle criterion and backstepping strategy control for a sensorless IM control scheme. The present paper is

*E-mail address: h.mellah@univ-bouira.dz
ISSN: 1791-2377
doi:10.25103/jestr.175.16

structured as follows: In Section 2, the IM's modelling is provided. Section three is intended for the description of the nonlinear Circle Criterion Observer (CCO). In Section 4, we present the theory of the HGO. In Section 5, we briefly recall the backstepping control technique. Finally, we end with a comparative simulation and interpretation of the obtained results, which allows us to draw conclusions from this work.

2. Mathematical Modelling of a Three-Phase IM

In the reference frame of the stator fixed (***α-β***) axis, the nonlinear model of the IM introduced in this work is given as follows:

$$\dot{x}(t) = f(x) + g(x)u(t) \tag{1}$$

$$y(t) = C\ x(t) \tag{2}$$

We note that the stator currents, the rotor's flux and angular velocity are the state variables. The measurable vector components are the currents $i_{s\alpha}$ and $i_{s\beta}$. The controller vector $u(t) = \left[u_{s\alpha}, u_{s\beta}, T_l\right]^T$.

Where:

$$f(x) = \begin{bmatrix} -\gamma i_{s\alpha} + \frac{\beta}{T_r}\varphi_{r\alpha} + \beta\omega\varphi_{r\beta} \\ -\gamma i_{s\beta} - \beta\omega\varphi_{r\beta} + \frac{\beta}{T_r}\varphi_{r\beta} \\ \frac{L_m}{T_r} i_{s\alpha} - \frac{1}{T_r}\varphi_{r\alpha} - \omega\varphi_{r\beta} \\ \frac{L_m}{T_r} i_{s\beta} + \omega\varphi_{r\alpha} - \frac{1}{T_r}\varphi_{r\beta} \\ \delta\left(\varphi_{r\alpha} i_{s\beta} - \varphi_{r\beta} i_{s\alpha}\right) - k_f\ \omega - \ k_l T_l \end{bmatrix},$$

$$g(x) = \begin{bmatrix} \frac{1}{\sigma L_S} & 0 \\ 0 & \frac{1}{\sigma L_S} \\ 0 & 0 \\ 0 & 0 \\ 0 & 0 \end{bmatrix}$$

Where: $\gamma = \frac{1}{\sigma}\left(\frac{1}{T_s} + \frac{1-\sigma}{T_r}\right)$, $\sigma = 1 - \frac{{L_m}^2}{L_s L_r}$, $k_l = \frac{n_p}{J}$, $k_f = \frac{f_{re}}{J}$,$\delta = \frac{n_p^2 L_m}{J L_r}$, $\beta = \frac{1}{L_m}\left(\frac{1-\sigma}{\sigma}\right) = \frac{1}{\sigma}\frac{m}{L_S L_r}$ and $\omega = n_p\,\Omega$. The following notations are introduced in order to simplify the mathematical equation forms: $x_1 = i_{s\alpha}\,, x_2 = i_{s\beta}\,, x_3 = \varphi_{r\alpha}\,, x_4 = \varphi_{r\beta}, x_5 = \Omega$.

The IM model has a nonlinearity that results from multiplying the rotor flux components by the angular velocity in the first four equations, and multiplying the state variables in the system's dynamic equation. This model becomes more complex when we take into account the variation of IM parameters such as rotor and/or stator resistances or inductances.

In this work, we focus on the nonlinearity caused by the change in rotor angular velocity, and we do not take into account the parameter variation. This kind of nonlinear model is commonly used for nonlinear control, condition monitoring, and fault diagnosis of electric motors [31-32]. However, for squirrel cage IM, all rotor-related parameters and states are not measurable, such as fluxes, resistances, and inductances. These states and parameters must be estimated as they are necessary for the control, monitoring, and diagnosis of the IM.

3. Nonlinear Observer Design Based on Circle Criterion

The structure of the nonlinear observer that utilizes the circle criterion adopted in this study to estimate of the rotor's flux and speed is the focus of this section.

Arcak and Kokotovic came up with the first version of this observer [22-23]. It works for continuous systems that can be split into linear and nonlinear parts, as long as the nonlinearities meet the sector property.

The advantage of this approach is to treat system nonlinearities with less restrictive conditions [22-24]. The essential theory and theorems used in the design of the nonlinear observer are illustrated as the following:

The nonlinear model (1) - (2) of the IM can be rewritten as:

$$\dot{x}(t) = A\ x(t) + \psi[u(t), y(t)] + N\varphi[M.x(t)] \tag{3}$$

$$y(t) = C\ x(t) \tag{4}$$

Where:

$x \in \mathbb{R}^n$ is the state variable, $y \in \mathbb{R}^p$and $u(t) \in \mathbb{R}^m$ is the output and the control input of the system. A, C and N are assumed to be known and constant matrices with appropriate dimensions provided that the system must be observable.

$\psi[u(t), y(t)]$ is an arbitrary real-valued vector that depends only on the system inputs and outputs, $u(t)$ and $y(t)$ respectively. The last term of the system (3) $\psi[M\ x(t)]$ which is a time-varying vector function that verifies the sector property, serves as the mathematical representation of the system's nonlinear component. We note that $\varphi(.)$ and $\psi(.,.)$ are locally Lipschitz.

A primary restriction stating that the nonlinear observer's function is a non-decreasing function $\varphi(.)$ is a requirement for its structure.

This restriction means that:

$$(\zeta - \xi)[\varphi(\zeta, t) - \varphi(\xi, t)] \geq 0\ \forall\ \zeta, \xi\ \epsilon\ R^+$$

If

$$(\zeta - \xi) = \eta \text{ and } [\varphi(\zeta, t) - \varphi(\xi, t)] = \varphi(\eta, t) \tag{5}$$

With:
$\varphi(\eta, t)$ is a nonlinearity function.
such as $\varphi(\eta, t)$: $[0\ + \infty[\times R^p \to R^p$ is said to appertain to the sector $[0\ + \infty[$ if $\eta\varphi(\eta, t) \geq 0$.

The previous equation is also equal to the following if $\varphi(\eta, t)$ is a continuously differentiable function [22], [23]:

$$\frac{d}{d\eta}\varphi(\eta, t) \geq 0\ \forall\ \eta\ \epsilon R \tag{6}$$

According to these restrictions, the observer will therefore be given as follows:

$$\dot{\hat{x}}(t) = A\hat{x}(t) + \psi[u(t), y(t)] + L[y(t), \hat{y}(t)] + N\varphi[M\hat{x}(t) + K_0(y(t) - \hat{y}(t))] \tag{7}$$

With:
$\hat{x}(t)$ and $\hat{y}(t)$ are the estimate of the state $x(t)$ vector and the output $y(t)$ vectors respectively.

M is a vector that satisfies the condition of linear independence with the output vertor C.

The state estimation error $e(t)$ is computed as a difference between the state $x(t)$ and state estimation $\hat{x}(t)$.

The gain matrices L and K_0 are determined as part of the nonlinear observer dynamic.

In order to carry out the previous observer, the main theorem and the conditions used in this work are recalled while adhering to the sector property as follows:

Theorem 1: According to [22] and [33] if we consider a nonlinear system of the form represented by equations (3) and (4) with the nonlinear part satisfying the equations of the circle criterion given by equations (5) and (6). If there exists a symmetric and positive definite matrix $S\epsilon\, R^{nxn}$ and a set of row vectors $K_0\epsilon\, R^{nxn}$ such that the following Linear Matrix Inequalities (LMI) are verified we have [18], [21]:

$$(A-LC)^T S + S^T(A-LC) + Q \leq 0 \tag{8}$$

$$SN + (M - K_0 C)^T = 0 \tag{9}$$

With:

$Q = \varepsilon I_n$: Positive gain matrix,
I_n : The $n \times n$ identity matrix,
ε: A positive real number.

From equations (7), (8) and (9), how the state observation error e(t) changes over time can be derived as follows:

$$\dot{e}(t) = (A-LC)e(t) + N\big[\varphi\big(Mx(t)\big) - \varphi\big(M\hat{x}(t)\big) + K_0(y(t) - \hat{y}(t))\big] \tag{10}$$

Let $\zeta = M.x(t)$, and $\xi = M.\hat{x}(t) + K_0(y(t) - \hat{y}(t)$ by taking $\eta = \zeta - \xi = (M - K_0 C)e(t)$, the equation (10) provides the dynamics of the state estimation error, which may be viewed as a function of the variable η and then $[\varphi(\zeta) - \varphi(\xi)] = \varphi(\eta, t)$. Thereafter, taking into consideration the prior outcome, the error dynamics become:

$$\dot{e}(t) = (A-LC)e(t) + N.h(\eta, t) \tag{11}$$

$$\eta = (M - K_0 C)e(t) \tag{12}$$

From equations (11) and (12), we notice that the design issue of the nonlinear estimator is similar to the stabilization of the dynamics error.

Using a CLF : $V = e^T Se$, the stability of the observer error dynamics is investigated.

The time derivative of the Lyapunov function is expressed as follows:

$$\dot{V} = \dot{e}^T se + e^T S\dot{e}^T \tag{13}$$

Equations (11) and (12) can be used to get the derivative of the Lyapunov function as follows:

$$(A-LC)^T S + S^T(A-LC) \leq -Q \tag{14}$$

and

$$SN = -(M - K_0 C)^T \tag{15}$$

The derivative of the Lyapunov function can be written as follows:

$$\dot{V} \leq -e^T Qe - 2.\eta^T \varphi(\eta, t) \tag{16}$$

The circle criterion has the benefit of handling the system's nonlinearities directly and with less limitation. However, this strategy introduces LMI's limitations. Fig. 1 represents the CCO's flowchart.

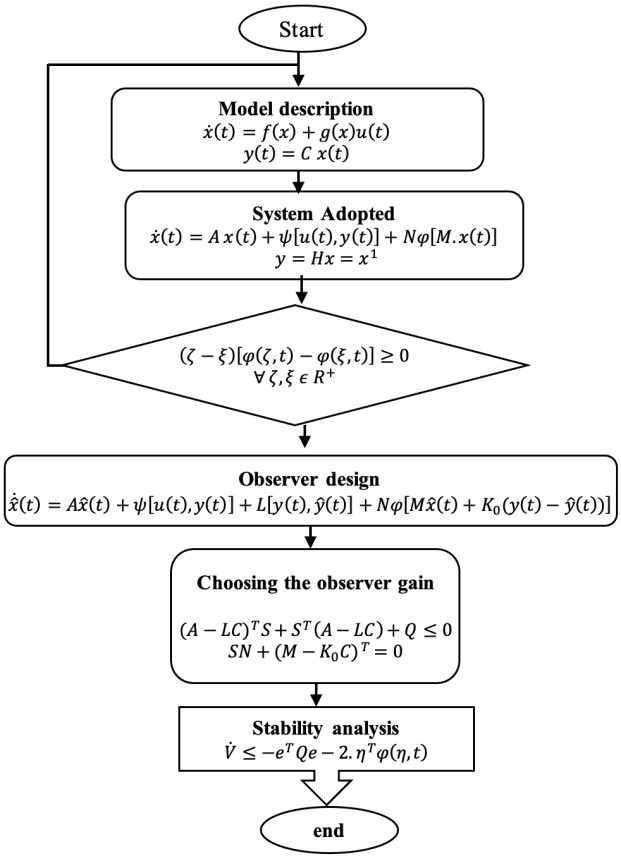

Fig. 1. Flowchart of the CCO

4. Nonlinear High Gain Observer

In the purpose to the design of the HGO the model of a uniformly observable nonlinear system is presented in the following manner [26]:

$$\dot{x} = f(x, u) + \varepsilon \tag{17}$$

$$y = Hx = x^1 \tag{18}$$

Where:

$$x = \begin{bmatrix} x^1 \\ x^2 \\ \vdots \\ x^q \end{bmatrix}; \chi = \begin{bmatrix} 0 \\ \vdots \\ 0 \\ \chi^{q-1} \\ \chi^q \end{bmatrix} \text{ and } f(x,u) = \begin{bmatrix} f_1(x^1, x^2, u) \\ f_2(x^1, x^2, x^3, u) \\ \vdots \\ f_{q-1}(x^1, x^2, \dots, x^{q-1}, u) \\ f_q(x, u) \end{bmatrix} \text{ and } H = \left[I_{n_1}, 0_{n_{1*}n_2}, \dots . 0_{n_{1*}n_{q_1}}\right]$$

With:$x \in \mathbb{R}^n, x^k \in \mathbb{R}^p$ for $k = 1,2,\dots,q$ and $n_1 \geq n_2 \geq \cdots n_q$. The input $\subset \mathbb{U}$a compact set of $\mathbb{R}^m$, the output $y \in \mathbb{R}^{n_1}$. $I_{n_1}$is the $n_1 \times n_1$ identity matrix. $0_{n_1 \times n_j}$ is the $n_1 \times n_l$ null matrix, $j \in \{2,\dots,q-1\}$. $\chi^k \in \mathbb{R}^{n_k}, k \in \{q-1, q\}$, each χ^k is a bounded real valued function that is unknown and dependent on uncertain parameters, in our situation, we suggest $\chi^k = 0$.

The design of a HGO of the system (17) and (18) requires the following hypotheses:

- There exist τ, λ where $0 < \tau \leq \lambda$ such that for all $k \in \{1,\dots,q-1\}, x \in \mathbb{R}^n, u \in U$ we have:

$$0 < \tau^2 I_{nk} \leq \left[\frac{\partial f_k(x^{1:k},u)}{\partial x^{k+1}}\right]^T \frac{\partial f_k(x^{1:k},u)}{\partial x^{k+1}} \leq \lambda^2 I_{nk}$$

Furthermore, we adopt that:

$$\text{Rank}\left(\frac{\partial f_k(x^{1:k},u)}{\partial x^{k+1}}\right) = n_{k+1}$$

- The function $f(x,u)$ is globally Lipchitz with respect to x, uniformly in u.

By respecting the conditions below, the design of the HGO of the system (17-18) can be written:

$$\dot{\hat{x}} = f(\hat{x}, u) - \theta \Lambda^{-1}(\hat{x}) \Delta_\theta^{-1} S^{-1} H^T \bar{H}(\hat{x} - x^1) \quad (19)$$

With $\Lambda^{-1}(\hat{x})$ is defined as the left inverse of block diagonal matrix $\Lambda(\hat{x})$:

$$\Lambda(\hat{x}) = blockdiag\left[I_{nk}, \frac{\partial f_k(x^{1:k},u)}{\partial x^{k+1}}, \dots, \prod_{i=1}^{q-1} \frac{\partial f_k(\hat{x},u)}{\partial \hat{x}^{k+1}}\right]$$

$$\Delta_\theta(\hat{x}) = blockdiag\left(I_{n_1}, \frac{1}{\theta} I_{n_1}, \dots, \frac{1}{\theta^{q-1}} I_{n_1}\right), \theta > 0$$

θ is a real value that represents the observer's unique design parameter.

S is a definite positive matrix, solution of the following algebraic Lyapunov equation:

$$S + A^T S + SA = H^T H \quad (20)$$

With: $H = [I_{n_1}, 0_{n_1}, \dots, 0_{n_1}]$,

$$\mathcal{A} = \begin{bmatrix} 0 & \bar{\mathcal{A}} \\ 0 & 0 \end{bmatrix}, \bar{\mathcal{A}} = blockdiag(I_{n_1}, 0_{n_1}, \dots, 0_{n_1}) \in \mathbb{R}^{n_1(q-1)}$$

It should be highlighted that equation (20) is independent of the system characteristics and that an analytical representation of the solution is possible.

$$S(i,j) = (-1)^{i+j} H_{i+j-2}^{j-1} I_{n1} \quad (21)$$

With:

$$H_j^i = \frac{j!}{i!\,(j-i)!} for\ 1 \leq i,j \leq q$$

According to these circumstances, the correction gain of equation (19) can be explicitly given as follows:

$$\theta \Lambda^{-1}(\hat{x}) \Delta_\theta^{-1} S^{-1} H^T = \begin{bmatrix} \theta H_1^q I_{n1} \\ \theta^2 H_2^q \left[\frac{\partial f_1}{\partial x^2}(x,u)\right]^- \\ \vdots \\ \theta^2 H_q^q \left[\Pi_{i=1}^{q-1} \frac{\partial f_k}{\partial x^{k+1}}(x,u)\right]^- \end{bmatrix} \quad (22)$$

It must be noted that the HGO design is fairly straight forward [34].

The diagram represented in Fig. 2 illustrates the HGO flowchart.

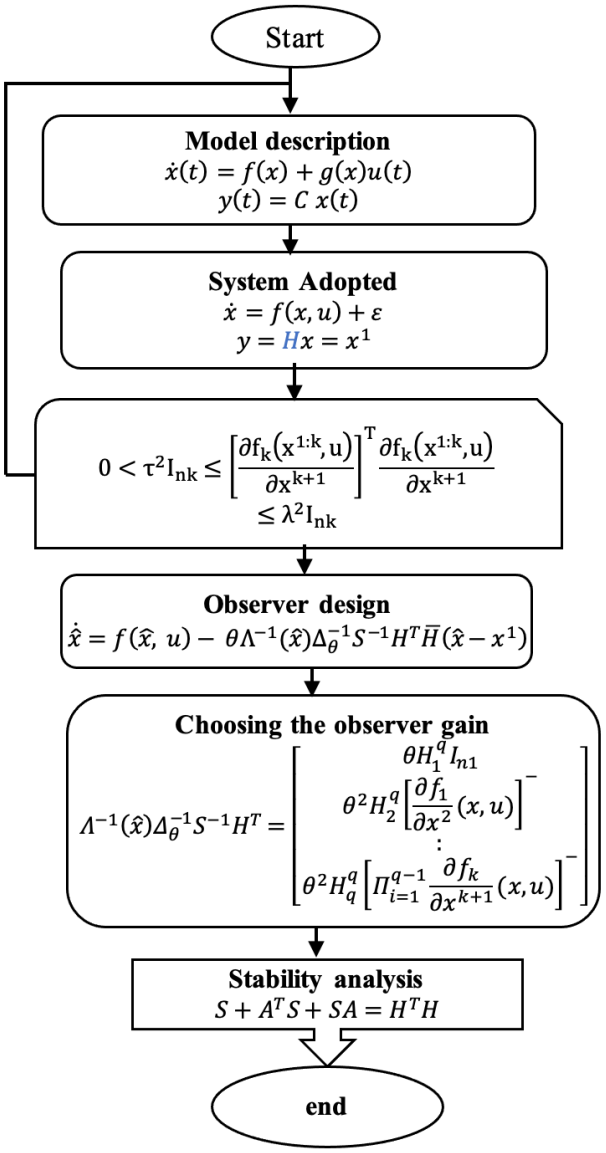

Fig. 2. flowchart of the HGO

5. Backstepping controller design for IM speed and flux

In this study, the sensorless control scheme based on backstepping control is used first with a circle criterion nonlinear state observer and then with a nonlinear HGO for the IM as depicted in Fig.3. The implementation of these speed-sensorless control approaches requires the observation of the unmeasured rotor flux linkage and speed based on the measurements of the stator's currents and voltage. Two stages make up the conception of the backstepping method.

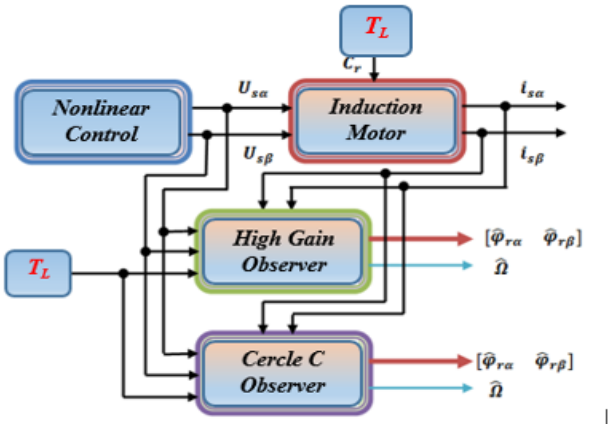

Fig. 3. Synoptic diagram of flux and velocity observation

➢ **Step 1**

To ensure accurate tracking performance, it is essential to design the controllers and specify the trajectories that the system would like to take.

We therefore define a desired trajectory, $y_{ref} = (\Omega_{ref}, \varphi_{ref}^2)$.

The reference trajectories for the flux module and rotor speed are denoted by Ω_{ref} *and* φ_{ref}^2. We mention $x_{5d} = \Omega_{ref}, x_{6d} = \varphi_{ref}^2$,with $\varphi_r^2 = \varphi_{r\alpha}^2 + \varphi_{r\beta}^2$

Where:

$$z_1 = x_{5d} - x_5 \tag{23}$$

$$z_2 = x_{6d} - x_6 \tag{24}$$

The tracking errors for flux magnitude and speed are represented by the variables $z_1$and z_2, respectively.

The following expressions represent the dynamic error:

$$\dot{z}_1 = \dot{x}_{5d} - \left[\frac{n_p L_m}{jL_r}(x_3 x_2 - x_4 x_1) - \frac{T_l}{j} - \frac{fre}{j}x_5\right] \tag{25}$$

$$\dot{z}_2 = \dot{x}_{6d} - \left[\frac{2L_m}{T_r}(x_3 x_1 + x_4 x_2)\right] + \frac{2}{T_r}x_6 \tag{26}$$

The definitions of the virtual control equations are as follows:

$$\alpha_1 = \left[\frac{n_p L_m}{jL_r}(x_3 x_2 - x_4 x_1)\right] \tag{27}$$

$$\beta_1 = \left[\frac{2L_m}{T_r}(x_3 x_1 + x_4 x_2)\right] \tag{28}$$

Equations (25) and (26) could be expressed as follows:

$$\dot{z}_1 = \dot{x}_{5d} - \alpha_1 + \frac{T_l}{j} + \frac{fre}{j}x_5 \tag{29}$$

$$\dot{z}_2 = \dot{x}_{6d} - \beta_1 + \frac{2}{T_r}x_6 \tag{30}$$

The candidate Lyapunov function chosen determines the dynamic stability of the errors:

$$v_1 = \frac{1}{2}[z_1^2 + z_2^2] \tag{31}$$

We derive the equation (31), we get:

$$\dot{v}_1 = z_1\dot{z}_1 + z_2\dot{z}_2 \tag{32}$$

By selecting the derivatives in the following manner, the Lyapunov function's negativity is obtained:

$$\dot{z}_1 = -c_1 z_1 \tag{33}$$

$$\dot{z}_2 = -c_2 z_2 \tag{34}$$

Virtual control may take the following forms:

$$\alpha_1 = c_1 z_1 + \dot{x}_{5d} + \frac{T_l}{j} + \frac{fre}{j}x_5 \tag{35}$$

$$\beta_1 = c_2 z_2 + \dot{x}_{6d} + \frac{2}{T_r}(x_{6d} - z_2) \tag{36}$$

c_1 and c_2 : positive gains that define the closed loop's dynamic.

The virtual control in equations (35–36) is selected to meet the control principles and serve as a reference for the subsequent stage in developing the backstepping control strategy.

➢ **Step 2**

In this stage, we define novel error dynamics as follows:

$$z_3 = \alpha_1 - \left[\frac{n_p L_m}{jL_r}(x_3 x_2 - x_4 x_1)\right] \tag{37}$$

$$z_4 = \beta_1 - \left[\frac{2L_m}{T_r}(x_3 x_1 + x_4 x_2)\right] \tag{38}$$

z_3 and z_4 are the novel dynamics of the errors.

We now present the dynamics errors in terms of z_3 and z_4.

$$\dot{z}_1 = -c_1 z_1 + z_3 \tag{39}$$

$$\dot{z}_2 = -c_2 z_2 + z_4 \tag{40}$$

The following equations (37) and (38) provide the errors dynamics.

$$\dot{z}_3 = \alpha_2 - \left[\frac{n_p K}{j}(x_3 u_{s\beta} - x_4 u_{s\alpha})\right] \tag{41}$$

$$\dot{z}_4 = \beta_2 - \left[2KR_r(x_3 u_{s\alpha} + x u_{s\beta})\right] \tag{42}$$

Where:

$$\alpha_2 = \dot{\alpha}_1 + \frac{n_p L_m}{jL_r}\left[\left(\gamma + \frac{1}{T_r}\right)(x_3 x_2 - x_4 x_1)\right] + \frac{n_p L_m}{jL_r}\left[n_p \Omega[(x_3 x_1 + x_4 x_2) + K x_6]\right]$$

$$\beta_2 = \dot{\beta}_1 + \frac{2L_m}{T_r}\left[\left(\gamma + \frac{1}{T_r}\right)(x_3 x_1 + x_4 x_2) - \frac{K}{T_r}x_6\right] + \frac{2L_m}{T_r}\left[n_p \Omega(x_3 x_2 - x_4 x_1) - \frac{L_m}{T_r}(x_1^2 + x_2^2)\right]$$

It is evident that equations (41) and (42) include the actual control elements. So, the final Lyapunov function could be constructed as:

$$v_2 = \frac{1}{2}[z_1^2 + z_2^2 + z_3^2 + z_4^2] \quad (43)$$

The final Lyapunov function's time derivative can be represented as follows by applying equations (39)–(42):

$$\dot{v}_2 = -c_1 z_1^2 + z_1 z_3 - c_2 z_2^2 + z_2 z_4 - c_3 z_3^2 \quad -c_4 z_4^2 + z_3 \left(z_1 + c_3 z_3 + \alpha_2 - \frac{n_p K}{j}\left(x_3 u_{s\beta} - x_4 u_{s\alpha}\right)\right) \quad + z_4 \left(z_2 + c_4 z_4 + \beta_2 - 2KR_r\left[\left(x_3 u_{s\alpha} + x_4 u_{s\beta}\right)\right]\right) \quad (44)$$

Where:

c_3 and c_4: positive design gains that define the closed loop's dynamic.

The Lyapunov function's negative is dependent on:

$$\dot{v}_2 = -c_1 z_1^2 - c_2 z_2^2 - c_3 z_3^2 - c_4 z_4^2 \leq 0 \quad (45)$$

As a result, we chose voltage control as follows:

$$c_3 z_3 + z_1 + \alpha_2 - \frac{n_p K}{j}\left(x_3 u_{s\beta} - x_4 u_{s\alpha}\right) = 0 \quad (46)$$

$$c_4 z_4 + z_2 + \beta_2 - 2KR_r\left[\left(x_3 u_{s\alpha} + x_4 u_{s\beta}\right)\right] = 0 \quad (47)$$

The following stator voltages are now determined as:

$$u_{s\alpha} = \frac{1}{x_6}\left[\frac{(\beta_2 + z_2 + c_4 z_4)}{2KR_r} x_3 - \frac{j}{n_p K}[\alpha_2 + z_1 + c_3 z_3] x_4\right] \quad (48)$$

$$u_{s\beta} = \frac{1}{x_6}\left[\frac{(\beta_2 + z_2 + c_4 z_4)}{2KR_r} x_4 + \frac{j}{n_p K}[\alpha_2 + z_1 + c_3 z_3] x_3\right] \quad (49)$$

6. Simulation Results

To illustrate the advantages of the proposed study, an induction machine with its proper characteristics is considered as presented in Table 1.

Table 1. Induction motor characteristics

Parameters	Symbols	Value Unit
Motor's power	Pa	1.5 KW
Stator voltage	U	220 V
Number of pair poles	p	2
Stator frequency	F	50 HZ
Load Torque	T_l	5 N.m
Stator inductance	Ls	0.274 H
Rotor inductance	Lr	0.274 H
Mutual inductance	L_m	0.258 H
Stator resistance	Rs	4.850 Ω
Rotor resistance	Rr	3.805 Ω
Rotor angular velocity	ω	297.25 rd/s
Friction coefficient	F_{re}	0.00114 N.s/rd
Inertia coefficient	j	0.0031 Kg^2/s

The simulation block diagram of the Integral Backstepping control combined with an observer nonlinear of the induction motor model is given in Fig. 4.

Two steps are necessary to carry out the simulation of the proposed scheme.

- Estimating the state variable vector based on the inputs (voltages) and outputs (currents)
- Use of the estimated variables to calculate the control

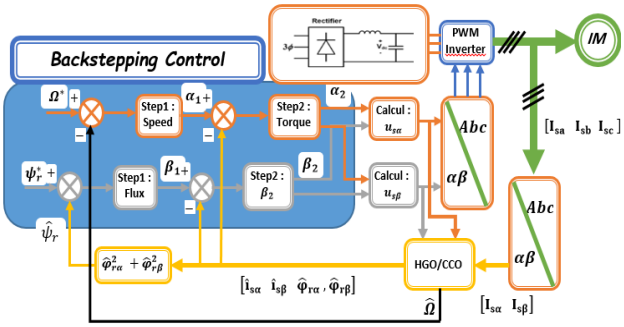

Fig. 4. Investigated sensorless control of induction motor drive using either High Gain observer and Circle criterion observer

In this section, a nonlinear sensorless control system applied to IM and backstepping control was designed and tested to compare the performance of the HGO and the CCO.

To evaluate the effectiveness of the two observers and therefore to draw an adequate comparison, four points were taken into consideration: trajectory tracking, low-speed operation, high-speed operation, and robustness to a load torque in both directions of rotation.

A nominal load torque of 5 Nm is applied to the IM from 2 to 4 seconds, with an increasing reference speed at 3 sec, causing a peak in the speed curve. At 5 sec, the reference speed is reversed, resulting in another peak in the speed curve. From 5.8 to 6.8 sec, a nominal load torque is applied again (-5 Nm). At 7 sec, the IM is forced to follow a reference speed to zero and then stabilize at 20 rad/sec, as shown in Fig. 3. Throughout these scenarios, the IM speed closely follows the reference.

Throughout the experiment, the flux vector's norm is constant and equal to 1 Wb.

Firstly, we start with the CCO for that, we must primarily solve the LMI conditions, the relations (8) and (9), using an LMI tool such as the LMI toolbox of the MATLAB software. The nonlinear observer gain matrices L and Ko obtained and that guarantee the system's stability are:

$$L = \begin{bmatrix} -132.3581 & -0.0000 \\ 0.0000 & -132.3581 \\ 1.7914 & -0.0000 \\ 0.0000 & 1.7914 \\ -0.0000 & 0.0000 \end{bmatrix}, K_1 = [5.4133 \quad -3.0149], K_2 = [3.0149 \quad -5.4133], K_3 = [-4.0085 \quad 5.0085], \text{and } K_4 = [5.0085 \quad -4.0085]$$

The appropriate Lyapunov matrix for the LMI feasibility test is:

$$P = \begin{bmatrix} 0.1787 & -0.0995 & 0.0029 & -0.0003 & -0.0330 \\ -0.0995 & 0.1787 & -0.0003 & 0.0029 & 0.0330 \\ 0.0029 & -0.0003 & 0.0871 & -0.0080 & -0.0000 \\ -0.0003 & 0.0029 & -0.0080 & 0.0871 & 0.0000 \\ -0.0330 & 0.0330 & 0.0000 & -0.0000 & -0.0000 \end{bmatrix}$$

With $\varepsilon = 0.04$.

Fig. 5 shows the measured and estimated torque of the two observers and the load torque. Fig. 6 shows the measured and

estimated speeds of the two observers and the reference speed. Fig. 7 shows the measured and estimated flux of the two observers and the reference flux. Fig. s 8 and 9 show the measured and estimated alpha and beta stator currents of the two observers, respectively.

According to Fig. 6, we notice that the two observers correctly estimate the rotor speed and ensure a good trajectory tracking. However, according to the zooms carried out during the rotor speed reversal shows that CCO is more efficient compared to the HGO.

After looking at the results represented in Fig.s 5 and 6, we can see that the backstepping control strategy and the CCO work well together, which is efficient and robust in terms of disturbance rejection (load torque) and perfect tracking of the rotor speed trajectory.

These findings lead us to the conclusion that sensorless control with the nonlinear backstepping approach offers an excellent solution for sensorless control of the IM.

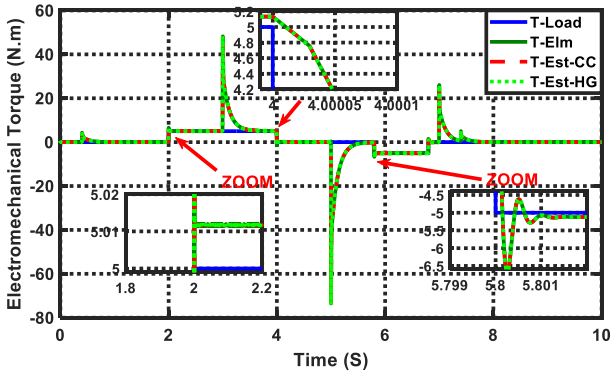

Fig. 5. Measured and observed electromechanical torque for a nonlinear observer based on the CCO and HGO

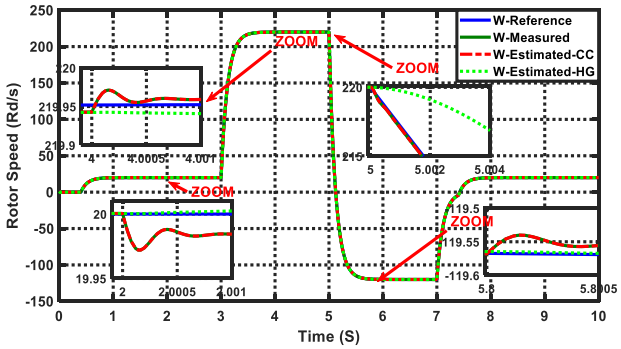

Fig. 6. Reference, measured and estimated rotor angular velocity for a nonlinear observer based on the CCO and HGO

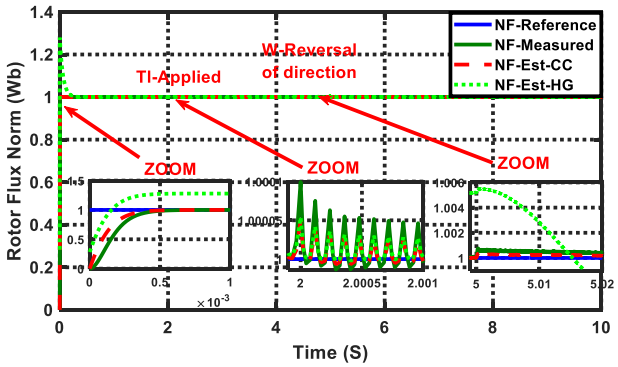

Fig. 7. Reference, measured and estimated rotor flux norm modulus for nonlinear observers based on the CCO and HGO

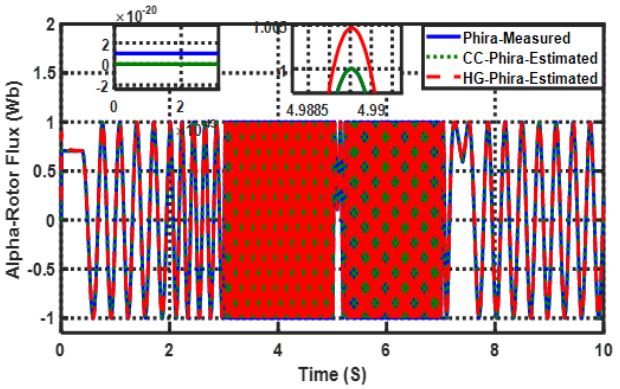

Fig. 8. Measured and estimated α-rotor flux components for a nonlinear observer based on the CCO and HGO

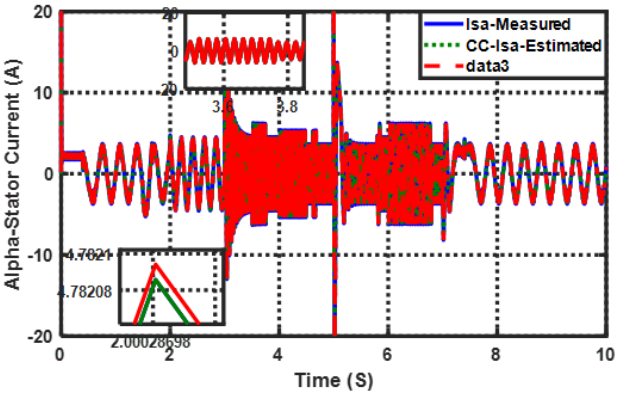

Fig. 9. Measured and estimated α-stator current components for a nonlinear observers based on the CCO and HGO

Analyzing Fig.s 5 and 6, we notice that the variables estimated by the CCO perfectly follow the measured variables. However, the variables estimated by HGO oscillate around the measured variables; this clearly shows the observer's efficiency.

Figures 8 and 9 show that the alpha stator current and alpha rotor flux are perfectly sinusoidal and follow the measured variables.

The results of the IM's nonlinear control employing a backstepping control combined with CCO under a load torque disturbance clearly demonstrate the rejection of this disturbance and the excellent tracking of the speed reference.

7. Conclusion

In this research, a comparative study was carried out between the observer based on the circle criterion and the high-gain observer in the control scheme using the backstepping control strategy. First, we note that the stability of the system is ensured by the control backstepping strategy based on the Lyapunov function and associating the two observers, despite the nonlinearity of the IM model. According to the simulation results, we can observe that the two observers correctly estimated the non-measurable parameters. However, the CCO observer presents better performances in terms of trajectory tracking, disturbance rejection, absence of oscillations, and especially during transient regimes. Moreover, we note that the ease of use of the HGO lies in the ease of its implementation and adjustment. Finally, we would like to emphasize that the proposed CCO observer handles the nonlinearities of the system directly with less restriction. Additionally, the observer is simple to implement and offers

satisfactory results for induction motors. However, this approach introduces constraints of the type LMI.

References

[1] F. Fathabadi and A. Molavi, "Black-box Identification and Validation of an Induction Motor in an Experimental Application," *Eur. J. Electr. Eng.*, vol. 21, no. 2, pp. 255–263, Jun. 2019, doi: 10.18280/ejee.210219.

[2] R. Abdelati and M. F. Mimouni, "Optimal control strategy of an induction motor for loss minimization using Pontryaguin principle," *Eur J Control*, vol. 49, pp. 94–106, Sep. 2019, doi: 10.1016/j.ejcon.2019.02.004.

[3] T. H. dos Santos, A. Goedtel, S. A. O. da Silva, and M. Suetake, "Scalar control of an induction motor using a neural sensorless technique," *Electr. Power Syst. Res.*, vol. 108, pp. 322–330, Mar. 2014, doi: 10.1016/j.epsr.2013.11.020.

[4] H. Mohamed, B. Abdelmadjid, and B. Lotfi, "Improvement of Direct Torque Control Performances for Induction Machine Using a Robust Backstepping Controller and a New Stator Resistance Compensator," *Eur. J. Electr. Eng.*, vol. 22, no. 2, pp. 137–144, Apr. 2020, doi: 10.18280/ejee.220207.

[5] R. Marino, S. Peresada, and P. Valigi, "Adaptive input-output linearizing control of induction motors," *IEEE Trans Automat Contr*, vol. 38, no. 2, pp. 208–221, 1993, doi: 10.1109/9.250510.

[6] S. Zaidi, F. Naceri, and R. Abdssamed, "Input-Output Linearization of an Induction Motor Using MRAS Observer," *Int. J. Adv. Sci. Techn.*, vol. 68, pp. 49–56, Jul. 2014, doi: 10.14257/ijast.2014.68.05.

[7] R. Tak, S. Y. Kumar, and B. S. Rajpurohit, "Estimation of rotor and stator resistance for induction motor drives using second order of sliding mode controller," *J.Eng.Sci.Tech.Rev*, vol. 10, no. 6, Dec. 2017, doi: 10.25103/jestr.106.02.

[8] R. Adireddy, K. Nanibabu, M. Ravindra, and K. V. S. Ramachandra Murthy, "Design of sliding mode controller for induction motor drive," *Mater Today Proc*, vol. 56, pp. 3237–3240, 2022, doi: 10.1016/j.matpr.2021.09.374.

[9] M. Fateh and R. Abdellatif, "Comparative study of integral and classical backstepping controllers in IFOC of induction motor fed by voltage source inverter," *Int J Hydrogen Energy*, vol. 42, no. 28, pp. 17953–17964, Jul. 2017, doi: 10.1016/j.ijhydene.2017.04.292.

[10] A. Benheniche and F. Berrezzek, "Integral Backstepping Control of Induction Machine," *Eur. J. Electr. Eng.*, vol. 23, no. 4, pp. 345–351, Aug. 2021, doi: 10.18280/ejee.230408.

[11] F. Berrezzek and A. Benheniche, "Backstepping Based Nonlinear Sensorless Control of Induction Motor System," *J. Eur. Syst. Autom.*, vol. 54, no. 3, pp. 495–502, Jun. 2021, doi: 10.18280/jesa.540313.

[12] Ph. Martin and P. Rouchon, "Flatness and Induction Motors," *IFAC Proceedings*, vol. 30, no. 27, pp. 451–454, Oct. 1997, doi: 10.1016/S1474-6670(17)41225-0.

[13] L. Fan and L. Zhang, "Fuzzy Based Flatness Control of an Induction Motor," *Procedia Eng*, vol. 23, pp. 72–76, 2011, doi: 10.1016/j.proeng.2011.11.2467.

[14] C. M. Kwan, F. L. Lewis, and K. S. Yeung, "Adaptive control of induction motors without flux measurements," *Automatica*, vol. 32, no. 6, pp. 903–908, Jun. 1996, doi: 10.1016/0005-1098(96)00012-X.

[15] N. F. Djagarov, H. A. Milushev, M. B. Bonev, Z. G. Grozdev and J. V. Djagarova, "Adaptive Vector Control of Induction Motor Drives," *2019 8th Int. Conf. Power Sci. Engin. (ICPSE)*, Dublin, Ireland, Dec. 2019, pp. 29-34, doi: 10.1109/ICPSE49633.2019.9041180.

[16] Y. Ren, R. Wang, S. J. Rind, P. Zeng, and L. Jiang, "Speed sensorless nonlinear adaptive control of induction motor using combined speed and perturbation observer," *Control Eng Pract*, vol. 123, p. 105166, Jun. 2022, doi: 10.1016/j.conengprac.2022.105166.

[17] F. Alonge, F. D'Ippolito, A. Fagiolini, and A. Sferlazza, "Extended complex Kalman filter for sensorless control of an induction motor," *Control Eng Pract*, vol. 27, pp. 1–10, May 2014, doi: 10.1016/j.conengprac.2014.02.007.

[18] T. Tamarozzi, P. Jiránek, and D. De Gregoriis, "A differential-algebraic extended Kalman filter with exact constraint satisfaction," *Mech Syst Signal Process*, vol. 206, p. 110901, Jan. 2024, doi: 10.1016/j.ymssp.2023.110901.

[19] A. Savoia, M. Mengoni, L. Zarri and D. Casadei, "A nonlinear Luenberger observer for sensorless vector control of induction motors," *Int. Aegean Conf. Electr. Mach. Pow. Electr. Electrom., Joint Confer.*, Istanbul, Turkey, Sep. 2011, pp. 544-549, doi: 10.1109/ACEMP.2011.6490657.

[20] W. EL Merrassi, A. Abounada, and M. Ramzi, "Performance analysis of novel robust ANN-MRAS observer applied to induction motor drive," *Int. J. Syst. Assur. Eng. Manag.*, vol. 13, no. 4, pp. 2011–2028, Aug. 2022, doi: 10.1007/s13198-021-01614-w.

[21] V. I. Utkin, "Sliding mode control design principles and applications to electric drives," *IEEE Trans. Ind. Electron.*, vol. 40, no. 1, pp. 23–36, Feb. 1993, doi: 10.1109/41.184818.

[22] M. Arcak and P. Kokotović, "Nonlinear observers: a circle criterion design and robustness analysis," *Automatica*, vol. 37, no. 12, pp. 1923–1930, Dec. 2001, doi: 10.1016/S0005-1098(01)00160-1.

[23] M. Arcak and P. Kokotović, "Feasibility conditions for circle criterion designs," *Syst Control Lett*, vol. 42, no. 5, pp. 405–412, Apr. 2001, doi: 10.1016/S0167-6911(00)00114-6.

[24] M. Arcak, "Circle-Criterion Observers and Their Feedback Applications: An Overview, "*Current Trends in Nonlinear Systems and Control. Systems and Control: Foundations & Applications*, Springer, pp. 3–14. doi: 10.1007/0-8176-4470-9_1.

[25] A. Kadrine, Z. Tir, O. P. Malik, M. A. Hamida, A. Reatti, and A. Houari, "Adaptive non-linear high gain observer based sensorless speed estimation of an induction motor," *J Franklin Inst*, vol. 357, no. 13, pp. 8995–9024, Sep. 2020, doi: 10.1016/j.jfranklin.2020.06.013.

[26] S. Hadj Saïd, M. F. Mimouni, F. M'Sahli, and M. Farza, "High gain observer based on-line rotor and stator resistances estimation for IMs," *Simul Model Pract Theory*, vol. 19, no. 7, pp. 1518–1529, Aug. 2011, doi: 10.1016/j.simpat.2011.03.006.

[27] A. Dib, M. Farza, M. M'Saad, Ph. Dorléans, and J. F. Massieu, "High gain observer for sensorless induction motor," *IFAC Proceedings*, vol. 44, no. 1, pp. 674–679, Jan. 2011, doi: 10.3182/20110828-6-IT-1002.02048.

[28] Z. Yin, Y. Zhang, C. Du, J. Liu, X. Sun, and Y. Zhong, "Research on Anti-Error Performance of Speed and Flux Estimation for Induction Motors Based on Robust Adaptive State Observer," *IEEE Trans. Ind. Electron.*, vol. 63, no. 6, pp. 3499–3510, Jun. 2016, doi: 10.1109/TIE.2016.2524414.

[29] A. Zemouche, F. Zhang, F. Mazenc, and R. Rajamani, "High-Gain Nonlinear Observer With Lower Tuning Parameter," *IEEE Trans Automat Contr*, vol. 64, no. 8, pp. 3194–3209, Aug. 2019, doi: 10.1109/TAC.2018.2882417.

[30] D. Astolfi, L. Marconi, L. Praly, and A. R. Teel, "Low-power peaking-free high-gain observers," *Automatica*, vol. 98, pp. 169–179, Dec. 2018, doi: 10.1016/j.automatica.2018.09.009.

[31] A. Ammar, A. Bourek, and A. Benakcha, "Nonlinear SVM-DTC for induction motor drive using input-output feedback linearization and high order sliding mode control," *ISA Trans*, vol. 67, pp. 428–442, Mar. 2017, doi: 10.1016/j.isatra.2017.01.010.

[32] R. Rahmatullah, A. Ak, and N. F. O. Serteller, "Design of Sliding Mode Control using SVPWM Modulation Method for Speed Control of Induction Motor," *Transp. Res. Proc.*, vol. 70, pp. 226–233, 2023, doi: 10.1016/j.trpro.2023.11.023.

[33] M. Arcak, "Certainty-equivalence output-feedback design with circle-criterion observers," *IEEE Trans Automat Contr*, vol. 50, no. 6, pp. 905–909, Jun. 2005, doi: 10.1109/TAC.2005.849257.

[34] Q. T.Dam, R. E. H. Thabet, S. A. Ali, F. Guérin, and H. A. Ghani, "A high-gain Observer Design for Nonlinear System with Delayed Measurements: Application to A Quadrotor UAV," *IFAC Proceedings*, vol. 56, no. 2, pp. 6739–6744, Nov. 2023, doi: 10.1016/j.ifacol.2023.10.379.

Nomenclature

Nomenclature	
A	State matrix
B	Input matrix
C	Output matrix
$c_1, c_2\ c_3, c_4$	positive gains that define the closed loop's dynamic
CCO	Circle Criterion Observer
CLF	Candidate Lyapunov Function
$e(t)$	State estimation error
f_{re}	Friction coefficient
$g(x), \varphi(\eta, t)$	Functions concerned circle criterion observer. Functions involved in circle criteria observer design
HGO	High-Gain Observer
IM	Induction motor
I_n	The $n \times n$ identity matrix.
$i_{s\alpha}, i_{s\beta}$	The stator currents components
J	Moment of inertia coefficient
K_0, L	Gain matrices of the nonlinear observer Nonlinear observer gain matrices
LMI	Linear Matrix Inequalities
L_m	Mutual inductance
L_s, L_r	Stator and rotor self-inductance
MRAS	Model Reference Adaptive System
n_p	Number of pair pole
P, N, M_o	Gains concerned circle criterion observer
Q	Positive gain matrix
R_r	Rotor resistance
R_s	Stator resistance
SM	Sliding Mode
S	Symmetric and positive definite matrix
S	Positive matrix solution of the algebraic Lyapunov equation
T_l	Mechanical load torque
T_l	Load torque
T_s, T_r	Stator and rotor time constants
$u(t)$	control vector
$u_{s\alpha}, u_{s\beta}$	$\alpha - \beta$ stator voltage component
V	Lyapunov function
v_1	candidate Lyapunov function
v_2	Final Lyapunov (function) ensuring the stability of the global system
$\dot{v}_2$	Final Lyapunov function's time derivative
$x(t), y(t)$	State and output vectors
z_1, z_2, z_3, z_4	Tracking errors in the backstepping controller
$\dot{z}_1$	dynamic error of rotor speed
$\dot{z}_2$	dynamic error of rotor flux modulus
$\dot{z}_3, \dot{z}_4$	Dynamic virtual variables' errors
α_1, β_1	Virtual controls
α_2, β_2	Output signals of the controllers of step two
ε	Positive real number
ζ, ξ	Real positive numbers
θ	Real value that represents the observer's unique design parameter.
σ	Constant of Blendel
τ, λ	Real positive numbers
$\hat{\cdot}$	Index of the estimated value
$\dot{\cdot}$	Index of the time differential operator (d/dt)
$\cdot_{ref}$	Reference index
χ	Bounded real valued function that is unknown and dependent on uncertain parameters
$\varphi(., t), \psi[.,.]$	Nonlinear functions
$\varphi_{r\alpha}, \varphi_{r\beta}$	Rotor flux components
Ω	Rotor speed
ω	Rotor angular velocity
ω	Rotor velocity